On Chaotic Pilot Wave Dynamics

Ruben Mason Carpenter

Under the direction of

Nicholas Zhixian Liu
Graduate student
MIT Mathematics Department

Research Science Institute

Abstract

A millimetric droplet can bounce indefinitely on a vibrating fluid bath and will self propel along the surface influenced by its underlying wave field, provided the vibration frequency is below the Faraday threshold. Every impact generates a new wave which adds towards the piloting wave field and simultaneously the previously generated wave kernels decay over time. Hence the dynamical system accumulates a total memory which correlates to the strength of the exerted wave force. We focus on the case where the droplet is also subject to a harmonic potential and its motion is constrained to a line. By analyzing the limit cycles in cases of high memory, we observe wave dominated trajectories resembling a growth-relaxation process that has been reported in previous literature studies in the absence of a spring force. Heuristically, as we progress towards chaotic behavior, we extend this type of behavior to unsteady walking dynamics where the quantized trajectory resembles a random walk. We numerically implement a variational method for approaching periodic orbits in a general flow, which we use for determining the nature of unstable periodic orbits arising in a random walk. We thus provide an alternate understanding of this behavior as transitioning between the neighborhoods of these unstable periodic orbits. Finally, we quantify the stability of these by calculating their Floquet multipliers, and we relate their magnitude to the emerging multimodal statistics in of the stationary points.

Summary

A droplet can jump indefinitely on a vibrating fluid bath without merging, and, when slightly nudged, it will initiate a horizontal movement across the surface of the fluid. Each impact generates a new wave in the total wave field and so its walking behaviour is modulated by the particle's surrounding waves, leading to either stable or completely chaotic trajectories. In the chaotic regime, this particle-wave system is known for exhibiting quantum mechanical-like behavior on a macroscopical scale. Examples of such behavior are quantum tunneling, emerging statistics and quantized trajectories, all of which have been observed experimentally. We work on the special case where the droplet is under the influence of a central force and its motion is restricted to one line. By implementing an algorithm for finding unstable periodic orbits and quantitatively assessing their stability, we seek to provide an alternative understanding for random walk like behavior that arises.

1 Introduction

1.1 Pilot wave theory

In 1997, Qian and Law [1] experimentally showed that a droplet may float without coalescenece on a vertically vibrating bath of fluid. At each impact of the droplet on the bath, a capillary wave propagates away from the droplet, exciting a field of standing Faraday waves [2], and thus adding to the existing field [3]. The first macroscopic realization, however, was not completed until 2005 by Couder et al. [4]: an oil droplet may *walk* across the surface of a vertically vibrating fluid bath, propelled by its own wave field. Figure 1 displays this physical phenomena. This horizontal movement has been understood because, for larger vibration frequency, the bouncing droplet is destabilized and thus even small nudge in the droplet's position will lead to the bouncing state being unstable and initiating a horizontal movement. The droplet, now called a *walker*, will now initiate a horizontal movement walking across the surface of the bath, propelled at each impact by the slope of its associated wave field, being directed by the *pilot waves* it generates. As the frequency of the bath vibration increases, so does the decay time of the Faraday waves. This yields a path memory from previous droplet impacts [5], leading to a macroscopic particle–wave interaction.

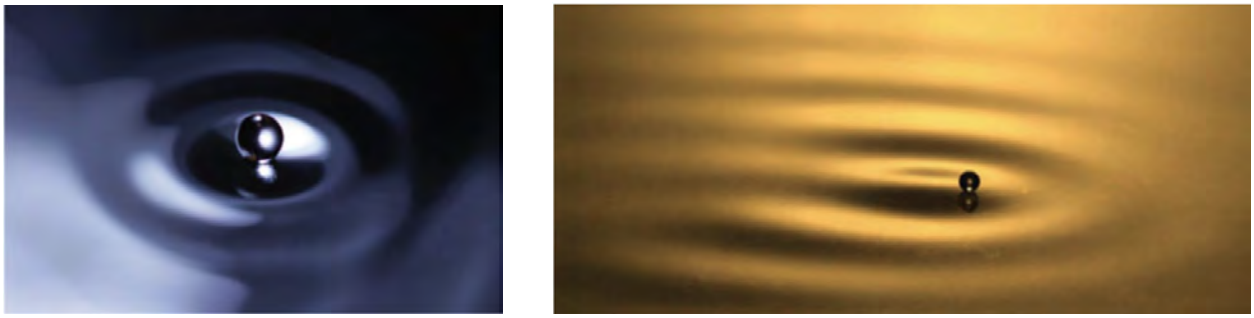

(a) (b)

Figure 1: (a) An oil droplet bouncing on a vibrating fluid bath (b) A self-propelled droplet walking laterally across the surface of a bath, resonant by it's interaction with the Faraday field. [6]

Perrard et al. [7] developed an experimental technique for encapsulating a small quantity of ferrofluid within a droplet, which enabled them to impart external forces to walkers directly. For instance, by applying a vertical magnetic field with a radial gradient, they were able to examine walker motion in a central harmonic potential. This was particularly interesting because, at moderate memory, a variety of periodic and quasi-periodic states arose when ranging over a large quantity of spring constants, including circles, lemniscates, trefoils and papillons. These periodic orbits were characterized in terms of their mean radius and angular momentum, and found to be roughly quantized in both quantities. In the high-memory regime, the walker was seen to switch intermittently between a number of these weakly unstable periodic orbits, *shadowing* them. In this sense, the chaotic motion can be considered as a superposition of periodic states. In other cases, such as in the Lorenz system, there also exists a classification of the UPO's [8].

1.2 Unstable periodic orbits in dynamical systems

Unstable periodic orbits (UPO's) play an important role in the analysis of a chaotic dynamical system; unstable periodic orbits can be seen as an islet of order in a dynamical system [9]. However, direct analysis of the transitions between them is tedious and often not precise because of the chaotic nature of the system. In fact, it wasn't until 2022 that an actual analysis of the shadowing in the Lorenz system was completed [10]. Hence, most research is actually done on the asymptotical statistics of the system.

In the frame of pilot mechanics, researching the underlying UPO's is a recurrent field of study. For instance, Oza et al. [11] discuss footprints of periodical orbits in classical pilot wave dynamics, justifying qualitatevely quantized behavior by unstability of periodic orbits. Further, Harris and Bush [6] have studied experimentally the multimodal statistics that arise within complex trajectories and quantized behaviour of the radius of curvature in a rotating frame. Their data is displayed in Figure 2.

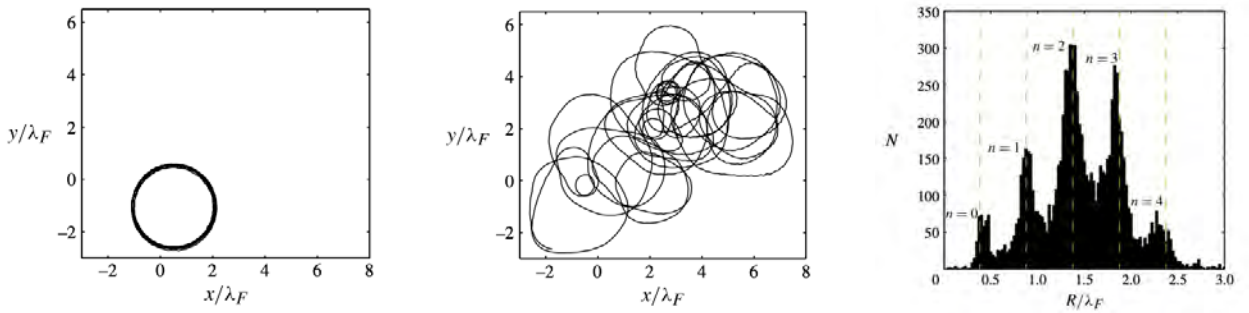

(a) (b) (c)

Figure 2: (a) Observed stable circular trajectory, in a rotating frame (b) Complex observed trajectory at the same rotation but with increased forcing, in the same rotating frame (c) Histogram of local radius of curvature [6]

In our study, we investigate a particle constrained in a one-dimensional wave under the influence of a harmonic potential. Motivated by the experimental data displayed in Figure 2 we also set foot on determining the periodic orbits in our dynamical system. We link the stability of periodic orbits to emerging multimodal statistics.

The rest of the paper is organized as follows: In Section 2 we set up the model we are analyzing. In Section 3 we describe the numerical tools we have implemented in order to perform our analysis. In particular, we discuss a variational method for determining periodic orbits, and then we discuss numerical implementation of Floquet theory for quantifying the instability. In Section 4 give an overview of the system's behaviour in terms of the memory, and in Sections 5 and 6 we present our data analysis.

2 A generalized Stroboscopic model

Trajectories of a droplet in a classical pilot wave system have usually been studied under the influence of a propelling wave force and an opposing drag force. Here, we consider an idealized one dimensional pilot wave system in which a droplet of mass m is propelled by

the guiding local slope of the wave field and resisted by drag force of coefficient D, with an added harmonic potential centered at the origin.

The stroboscopic approximation given by Oza et al. [12] is the framework of our numerical investigation. The resulting model, as published in 2013, is displayed in Definition 2.1 in its full generality.

Definition 2.1 (Oza et al. [12])**.** Assume a droplet of mass m is being propelled by it's self generated pilot wave. Then, its position $\mathbf{x}_p$ can be approximated by the following integro-differential equation

$$m\frac{d^2\mathbf{x}_p(t)}{dt^2} + D\frac{d\mathbf{x}_p(t)}{dt} = -\frac{F}{T_F}\nabla\int_{-\infty}^{t}\frac{\mathcal{H}(\mathbf{x}_p(t)-\mathbf{x}_p(s))}{|\mathbf{x}_p(t)-\mathbf{x}_p(s)|}\cdot(\mathbf{x}_p(t)-\mathbf{x}_p(s))e^{\frac{-(t-s)}{T_F M_e}}ds.$$

Here F is the wave force averaged out over an oscillation period of length T_F, $\mathcal{H}$ denotes the wave kernel and Me the path memory.

In our study we project Definition 2.1 onto one dimension and add a central harmonic potential. The governing equations then read as

$$m\frac{d^2x_p}{dt^2} + D\frac{dx_p}{dt} = -F\frac{\partial h(x,t)}{\partial x}\bigg|_{x=x_p} - Kx_p, \tag{1}$$

$$h(x,t) = \frac{1}{T_F}\int_{-\infty}^{t}\cos(x(t)-x(s))e^{-\frac{(t-s)}{T_F M_e}}ds, \tag{2}$$

where we have made the analysis considerably more treatable by choosing the wave kernel $\mathcal{H}$ to be the cosine function [13].

Equations 1 and 2 can be understood visually from the horizontal force balance given in Figure 3. In 2013, both Oza et al. [12] and Molaçek and Bush [14] concluded that we can neglect the droplet's vertical movement by averaging out over the droplet's vertical bouncing period. Thus, the total wave height $h(x,t)$ in Equation 2, is calculated through continuous integration of the multiple waves that are generated by the particle after every impact.

In the spirit of nondimensionalization [12], we now define a non dimensional parameter space in a rescaled time frame. The main definitions are the following.

Definition 2.2 (Inertia)**.** The *inertia* k_0 of the droplet is defined as $k_0 = \frac{m}{D\tau_0}$

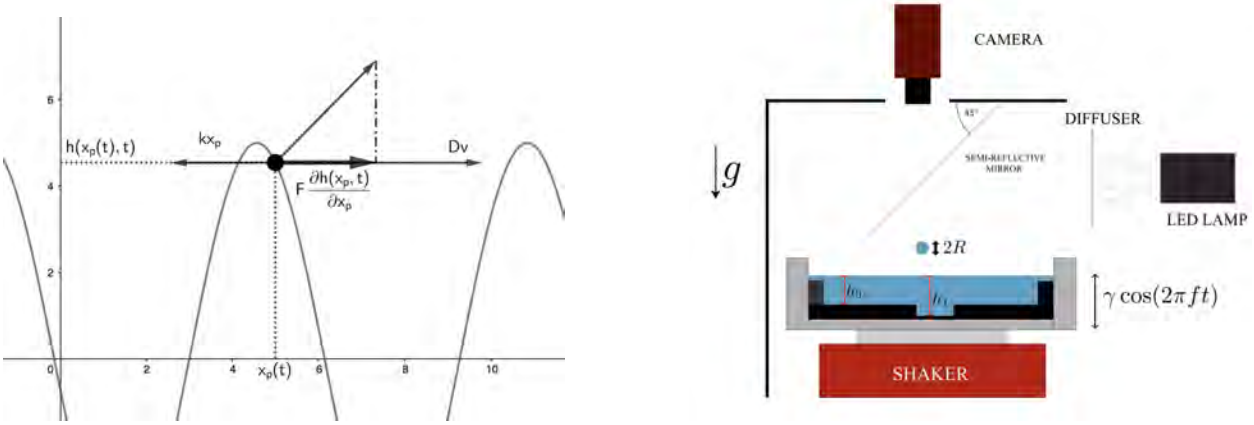

(a) (b)

Figure 3: (a) Horizontal force balance of the droplet at time t and position $x_p(t)$. The forces that are captured are: an attractive spring force $kx_p(t)$ centered at the origin, a drag force of modulus Dv in the same direction of the velocity and the x - component of the wave force averaged over one jump. (b) Experimental setup by [15]. A droplet of radius R bounces on a fluid bath vibrating at a frequency of f

Definition 2.3 (Memory)**.** The *memory* of system 4 is defined as $\Gamma = 1 - \mu$, where $\mu = \frac{1}{M_e}$

Definition 2.4 (Spring constant)**.** The *spring constant* is defined as $k = \frac{K}{D}$

Under Definitions 2.2, 2.3 and 2.4, we combine Equations 1 and 2 yielding

$$\kappa_0 \ddot{x}_p(t) + \dot{x}_p(t) = -kx_p(t) + \int_{-\infty}^{t} \sin(x_p(t) - x_p(s)) e^{-\mu(t-s)} ds. \tag{3}$$

The definition of each of k, k_0, μ which will adopt a physical significance later on.

Recently Durey [16] transformed an expression similar to Equation 3 into a system of three differential equations. Following his footsteps, we motivate the following definitions.

Definition 2.5 (Local wave amplitude)**.**

$$a(t) := h\left(x(t), t\right) = \int_{-\infty}^{t} \cos\left(x_p(t) - x_p(s)\right) e^{-\mu(t-s)} ds,$$

Definition 2.6 (Local wave slope)**.**

$$b(t) := \frac{\partial a}{\partial x} = -\int_{-\infty}^{t} \sin(x_p(t) - x_p(s)) e^{-\mu(t-s)} ds,$$

By differentiating Equation 2.5 and 2.6 with respect to time, substituting $\dot{x} = v$ and b into 3 and writing $h(x,t)$ in terms of $a(t)$ and $b(t)$, we rewrite the integro-differential Equation in terms of the position x, the velocity v, the local wave amplitude a and the local wave slope b in the following manner.

$$\begin{aligned} \dot{x} &= v \\ \dot{v} &= -\frac{1}{k_0}(kx + v + b) \\ \dot{a} &= 1 - \mu a + vb \\ \dot{b} &= -va - \mu b, \end{aligned} \tag{4}$$

In what follows we consider the spring constant k to be positive. The case of a repelling spring force is left for further exploration elsewhere.

3 Numerical methods

We can write our system in vector form

$$\frac{d\mathbf{y}}{dt} = f(\mathbf{y}) = Df(\mathbf{y}_0, t)\mathbf{y}$$

where we have defined

$$\mathbf{y}(t) = \begin{bmatrix} x \\ v \\ a \\ b \end{bmatrix} \quad \text{and} \quad Df(\mathbf{y}_0, t) := \begin{bmatrix} 0 & 1 & 0 & 0 \\ -\frac{k}{k_0} & -\frac{1}{k_0} & 0 & -\frac{1}{k_0} \\ 0 & b(t) & -\mu & v(t) \\ 0 & -a(t) & -v & -\mu \end{bmatrix},$$

for the initial condition $\mathbf{y}_0 = \mathbf{y}(0)$

In our research, we numerically solve Equations (4) by using a Runge Kutta 4 method. We wish to understand chaotic trajectories from the fundamental periodic orbits in the system. For this we need to i) determine the periodic orbits, and then ii) we need to quantify their stability.

Subsection 3.1 explains the numerical method employed for step 1, and subsection 3.2 presents the background for a floquet multiplier analysis. To find an initial guess when

scouting of these periodic orbits, we take the Poincaré section $\mathcal{S}$ through $v = 0$. If we require the position to satisfy $x(T + t) = x(t)$, we know by Rolle's theorem that there must be a moment in which $\dot{x} = v = 0$. Hence every periodic orbit must cross $v = 0$, an thus this section $\mathcal{S}$ is so powerful.

3.1 Variational principles for locating periodic orbits in differential equations

Consider a general dynamical system of the form $\frac{d\mathbf{y}}{dt} = v(\mathbf{y})$. In this method, we start with an orbit which is approximately periodic and toggle it to approach the actual periodic orbit $\mathcal{O}$ in the limit $t \to \infty$. We require an initial guess for:

- A set of n points $\{s_1, \ldots, s_n\}$ on a differentiable curve $\tilde{\mathbf{y}} \in \mathcal{L}$ such that parametrized under $s \in [0, 2\pi]$, such that

  $$\tilde{\mathbf{y}}_n = \tilde{\mathbf{y}}(t_n).$$

  The orbit $\mathcal{O}$ in the form $s \in \{s_1, \ldots, s_n\} \in [0, 2\pi]^n$ such that $\tilde{\mathbf{y}}(s_n) = \tilde{\mathbf{y}}_n$.

- A scaling factor $\lambda = \frac{T_p}{2\pi}$ for the proportion between the periods of $\mathcal{O}$ and $\mathcal{L}$. This ensures that the loop increment in $\mathcal{L}$ is proportional to it's counterpart in $\mathcal{O}$.

Denote by $\tilde{v}$ the velocity $\tilde{v}(\tilde{\mathbf{y}}) = \frac{d\tilde{\mathbf{y}}}{ds}$. Using a Newton–Raphson descent [17, 18], we alter $\tilde{\mathbf{y}}$ so that $\tilde{v}$ points in the same direction as $v(\mathbf{y})$. Analytically, we are monotonically decreasing the cost functional

$$F^2(\tilde{\mathbf{y}}) = \frac{1}{2\pi} \oint_{\mathcal{L}(\tau)} \left(\tilde{v}(\tilde{\mathbf{y}}) - \lambda v(\tilde{\mathbf{y}})\right)^2 d\tilde{\mathbf{y}},$$

and thus in the limit $t \to \infty$, we get $\mathcal{L} = \mathcal{O}$.

This can be done by deforming the parametrized loop $\tilde{\mathbf{y}}(s, \tau) \in \mathcal{L}$ according to the partial differential equation

$$\frac{\partial^2 \tilde{\mathbf{y}}}{\partial \tau \partial s} - \lambda A \frac{\partial \tilde{\mathbf{y}}}{\partial \tau} - v \frac{\partial \lambda}{\partial \tau} = \lambda v - \tilde{v}, \tag{5}$$

where τ denotes a ficticious time deformation parameter.

3.2 Quantifying the unstability of periodic orbits

Now that we are able to numerically find the periodic orbits, we are interested in using them for understanding the chaotic trajectories. For this we first quantify how unstable they are. To assess the stability of a periodic orbit $\mathcal{O}$ with period T, we are interested in understanding a trajectory starting at an initially perturbed vector $\mathbf{y}_0 + \Delta\mathbf{y}_0$ for a point $\mathbf{y}_0 \in \mathcal{O}$. We appeal to Lemma 3.1, the proof of which can be found in [19].

Lemma 3.1. *Let $\Delta\boldsymbol{y}(t) = f^t(\boldsymbol{y}_0 + \Delta\boldsymbol{y}_0) - f^t(\boldsymbol{y}_0)$, and define the Jacobian matrix J_t by $\Delta\boldsymbol{y}(t) = J_t\Delta\boldsymbol{y}_0$. Then*

$$\frac{dJ_t}{dt} = Df(\boldsymbol{y}_0, t)J_t. \tag{6}$$

Given $\mathbf{y}_0 \in \mathcal{O}$, the matrix $Df(\mathbf{y}_0, t)$ is periodic, and thus we get an instance of Floquet theory.

Formal framework of Floquet theory

Following [19, 20], We briefly discuss some basic Floquet theory needed to quantify the stability of periodic orbits in a dynamical system.

Theorem 3.2 (Floquet's theorem)**.** *Let A be a T-periodic function that is continuous on all of $\mathbb{R}$. If Φ is a fundamental matrix solution to an equation of the form $\dot{x} = A(t)x$, then Ψ can be written in the form:*

$$\Psi(t) = P(t)e^{Qt}$$

where P is a T-periodic matrix and Q is a constant matrix. Further,

$$\det \Psi(x) = \det \Psi(x_0) \exp\left(\int_{x_0}^{x} \operatorname{Tr} A(\xi)d\xi\right).$$

Given that $\Psi(T + t) = e^{QT}\Psi(t)$, we are motivated to define the following.

Definition 3.1 (Monodromy matrix)**.** The monodromy matrix is the normalized fundamental solution and satisfies

$$\dot{\Psi}(t) = A(t)\Psi(t) \text{ and } \Psi(0) = I_n.$$

The effect of the monodromy matrix is hence characterised by the following two.

Definition 3.2 (Floquet multipliers)**.** The *Floquet multipliers* or characteristic multipliers are defined as the eigenvalues $\lambda_1, \lambda_2, \ldots, \lambda_n$ of $\Psi(T)$, or equivalently, the eigenvalues of e^{QT}.

Definition 3.3 (Floquet Exponents)**.** A *Floquet exponent* is a $\mu \in \mathbb{C}$ such that $e^{\mu T}$ is a Floquet multiplier.

Finally, we also present the following result that can be found in [19].

Lemma 3.3. *If a nonlinear system has a periodic solution, then one of it's Floquet multipliers is exactly 1. Conversly, if $\Psi(t)$ has an eigenvalue of 1 then there is an orbit of period t containing $\boldsymbol{y}_0$.*

Numerical calculation of Floquet multipliers

In order to find the Floquet multipliers it is necessary to solve Equation 6 for J_t, and then evaulate the eigenvalues after a period has elapsed. A standard way of Equation 6 is by solving for the trajectory and the Jacobian at the same time. In our case, we would be solving the following system of 20 differential equations:

$$\mathbf{y}(t_{n+1}) = Df(\mathbf{y}_0, t_n)\mathbf{y}(t_n) \text{ and } J_{t_{n+1}} = Df(\mathbf{y}_0, t_n)J_{t_n}.$$

This is useful because we only require an initial point an the period as inputs, and for fairly stable orbits we get accurate results. However, when the orbit is considerably unstable, the numerical error propagates quickly and leads to inaccurate solutions. We link this uncertainty to to floating point error and truncation error. Thus we propose a new numerical method for calculating the Floquet multipliers of J_T. by solving a time-dependent equation.

The output of the variational method described in Section 3.1 is in the form

$$(\{\mathbf{y}_1, \mathbf{y}_2, \ldots, \mathbf{y}_n\}, \lambda) \text{ for } \mathbf{y}_i \in \mathbb{R}^4, 1 \leq 1 \leq n$$

where the points $\{\mathbf{y}\}_{1 \leq i \leq n}$ lie close to a periodic orbit $\mathcal{O}$. Since we have our periodic orbit on a grid, it is wise to use the Adams-Bashforth Two-Step method [21] for solving Equation 6.To

find the time steps Δt_n, we can approximate them using a reverse Adams-Bashforth method by solving for the already known trajectory as follows:

$$\mathbf{y}_{n+1} - \mathbf{y}_n = \left(\frac{3}{2} f(\mathbf{y}_n, t_n) - \frac{1}{2} f(\mathbf{y}_{n-1}, t_{n-1}) \right) \Delta t_n,$$

where we determine both vectors $\mathbf{y}_{n+1} - \mathbf{y}_n$ and $\frac{3}{2} f(\mathbf{y}_n, t_n) - \frac{1}{2} f(\mathbf{y}_{n-1}, t_{n-1})$ from the input, so we can get close to Δt_n by averaging out the proportions between each components of the vectors in the left and right hand side.

4 The route to chaos

As shown in Definitions 2.2, 2.3 and 2.4, the system parameters k, k_0, μ can be altered relative to those corresponding to the physical fluid system. In this section, we will give an overview of the dynamics that arise when solving Equations 4 over asymptotic values of Γ in the parameter space. We begin by studying the effect on the stabilty of the fixed point, and then we qualitatively assess the behaviour of the particles trajectory for large memory.

4.1 Linear stability analysis of the bouncing state

In Lemma 4.1 we state the bouncing state of the dynamical system where the point does not move. We begin our investigation by characterizing its stability in terms of the memory parameter Γ.

Lemma 4.1. *The dynamical system displayed in Equation 4 has a unique fixed point at* $(x_p, v, a, b) = (0, 0, \frac{1}{1-\Gamma}, 0)$.

The following result, which is not surprising given the definition of μ, allows us to restrict $0 < 1 < \mu$.

Lemma 4.2. *For* $\mu > 1$ *every trajectory eventually converges to the bouncing state.*

Proof. Consider the Lyapunov function

$$\mathbb{E}(x, v, a, b) = \frac{1}{2}\left(kx^2 + k_0v^2 + \mu(a - \frac{1}{\mu})^2 + \mu b^2\right).$$

Differentiation with respect to time t yields

$$\frac{d\mathbb{E}}{dt} = -\left((v + b)^2 + (\mu^2 - 1)b^2 + (\mu a - 1)^2\right)$$

for trajectories following Equations 4. When $\mu \geq 1$, then $\frac{d\mathbb{E}}{dt} \leq 0$ with equality only at the bouncing state. Thus it will be a global attractor. □

We follow the linear stability analysis taken by Oza et. al [12] on two dimensional pilot wave dynamics by applying a perturbation $x(t) = x_{eq}(t) + \epsilon x_1(t)H(t)$ to the stationary solution. Here $H(\bullet)$ is the Heaviside function introduced to apply a perturbation only for $t > 0$, and ϵ is assumed small.

Taking the Laplace transform of Equation 3 yields:

$$\mathcal{L}(x_1)[s] = \frac{k_0 s\dot{x}_p(0) - k_0 x_p(0) - x_p(0)}{s^2k_0 + s + k - \frac{1}{\mu} + \frac{1}{\mu+s}}. \tag{7}$$

Evidently x_{eq} is stable if $x_1(t)$ decays to zero. Therefore, any exponential growth rates r must have negative real part, which implies that the Laplace transform of frequency s should never diverge when $\mathrm{Re}(s) > 0$. Thus, we assess the stability of x_{eq} by studying the poles $s \in \mathbb{C}$ of $\mathcal{L}(x_1)[s]$. Equation 7 has a singularity at $s = -\mu < 0$. The rest are given by the roots of the polynomial:

$$p(s) := (\mu + s)\left(s^2k_0 + s + k - \frac{1}{\mu} + \frac{1}{\mu + s}\right) = \mu k_0 s^3 + (\mu^2 k_0 + \mu)s^2 + (\mu k + \mu^2 - 1)s + \mu^2 k,$$

Clearly p always has a negative root in $(0, 1)$, so it suffices to study the limit case when the other two roots are conjugate imaginary roots. It is straightforward to check that this happens exactly when $k_0\mu^3 + \mu^2 - \mu(k_0 - k) - 1 = 0$. This means that for every $k, k_0 > 0$, there exists a $\mu_s(k, k_0)$ such that for $\mu > \mu_s(k, k_0)$ the fixed point is stable, and is unstable otherwise.

Note that $-\frac{1}{k_0\mu}p(s)$ is in fact the characteristic polynomial of matrix $Df(\mathbf{y}_0, t)$.

4.2 Wave dominated behaviour

To better understand the effect of memory on the droplet's behaviour, in Figure 5 we plot x against v (first column), a against b, second column, and x against t (third column) for constant inertia and spring force and increasing memory. For low values of memory Γ, we report behaviour akin to that of a simple harmonic oscillator, and as we increase memory the particles trajectory is more strongly influenced by oscillations in it's corresponding wave field as the exerted wave force becomes stronger. Eventually the limit cycles destabilize and culminate in a random walk like behaviour.

In the rest of our study, we restrict our attention to irregular walking displayed in Figure 5 (j), (k), (l). Before moving on, we provide a physical explanation for quantized behaviour in the particles position, which we illustrate in a simple case. The limit cycle in Figure 4 elucidates the concept of a growth-relaxation process. This behaviour can be explained physically as follows: the particle's velocity is close to zero for a long period of time, during which the wave builds up beneath the particle. Eventually the wave force exceeds the drag force, pulling the droplet towards a neighbouring minimum in the wave field. Here the confining surrounding of the waves cause the droplet to slow down significantly. This process then repeats.

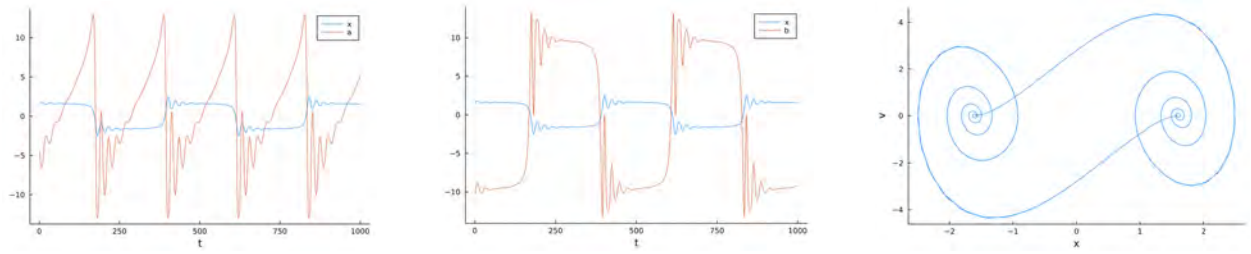

(a) (b) (c)

Figure 4: Numerical solutions for the parameter case $(k, k_0, \mu) = (6, 1, 0.005)$ plotted over 400 time steps. (a) Position $x(t)$ (blue) against local wave amplitude $a(t)$ (red) over a scaled time period (b) Position $x(t)$ (blue) against local wave slope $b(t)$ (red) over a scaled time period (c) Velocity v against position x.

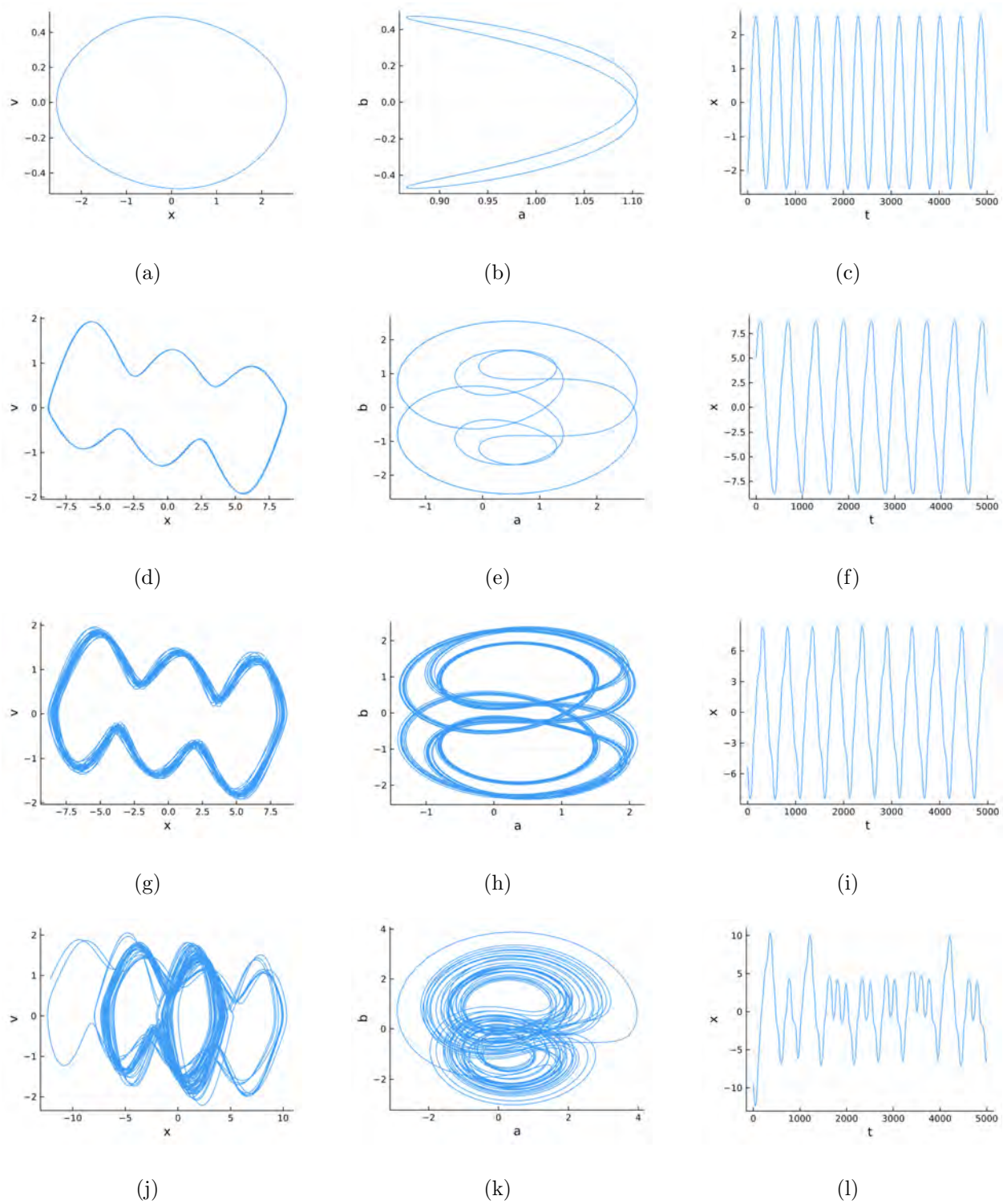

(a) (b) (c)

(d) (e) (f)

(g) (h) (i)

(j) (k) (l)

Figure 5: Numerical solutions plotting position over 400 time steps (a), (b), (c) $(k, k_0, \mu) = (0.1, 2, 0.9)$ (d), (e), (f) $(k, k_0, \mu) = (0.1, 2, 0.3)$ (g), (h), (i) $(k, k_0, \mu) = (0.1, 2, 0.23)$, (j), (k), (l) $(k, k_0, \mu) = (0.1, 2, 0.2)$.

5 Results

To study random walk like behavior, we seek a parameter regime characterised by trajectories where walkers switch between UPO's chaotically. Hence, we study the cases of low inertia k_0 and high Γ.

We now present a sample of our results, having applied the tools discussed in Section 3.

5.1 The case $(k, k_0, \mu) = (0.04, 0.6, 0, 22)$

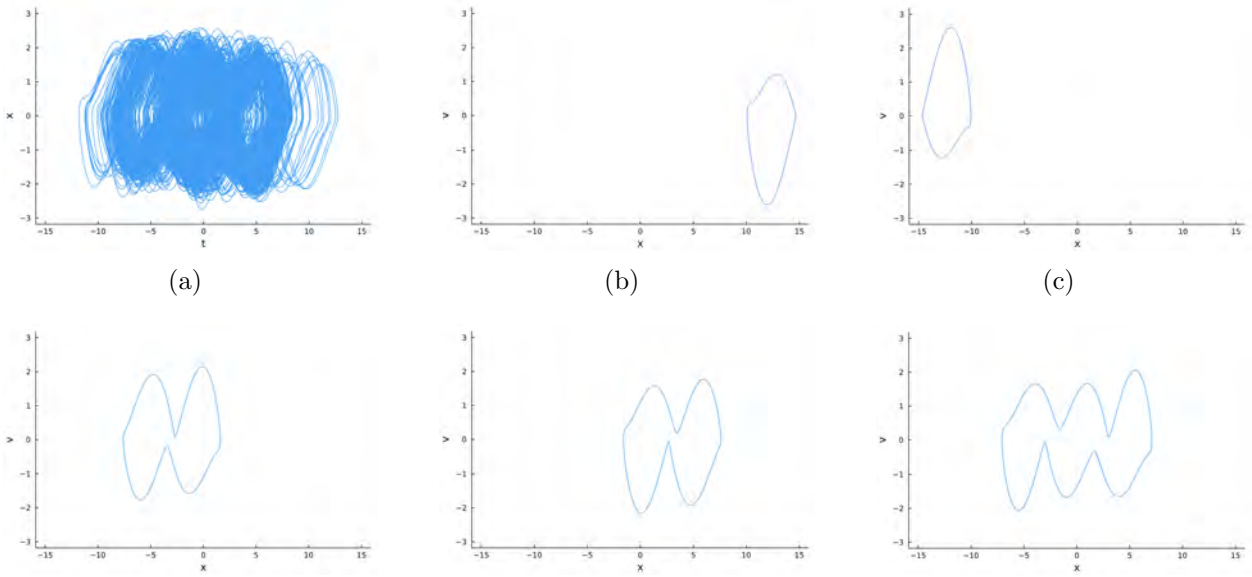

(a) (b) (c)

(d) (e) (f)

Figure 6: Numerical solution for the case $(k, k_0, \mu) = (0.04, 0.6, 0, 22)$, all plots being x against v (a) Whole trajectory (b) Orbit $\mathcal{O}_1$, (b) Orbit $\mathcal{O}_2$, (b) Orbit $\mathcal{O}_3$, (b) Orbit $\mathcal{O}_4$, (b) Orbit $\mathcal{O}_5$

Periodic orbit	Floquet multipliers	Largest Floquet multiplier
$\mathcal{O}_1$	7.1997, 1.0003, 0.9985, 4.3684e-15	7.1995
$\mathcal{O}_2$	7.1997, 1.0003, 0.9985, 4.3684e-15	7.1995
$\mathcal{O}_3$	4.0760, 1.0078, 0.9998, 7.9876e-14	4.0760
$\mathcal{O}_4$	4.0760, 1.0078, 0.9998, 7.9876e-14	4.0760
$\mathcal{O}_5$	15.0802, 1.0491, 1.1749, -5.8714e-15	15.0802

Table 1: Numerically computed Floquet multipliers using the method discussed in Subsection 3.2

5.2 The case $(k, k_0, \mu) = (0.05, 0.6, 0.22)$

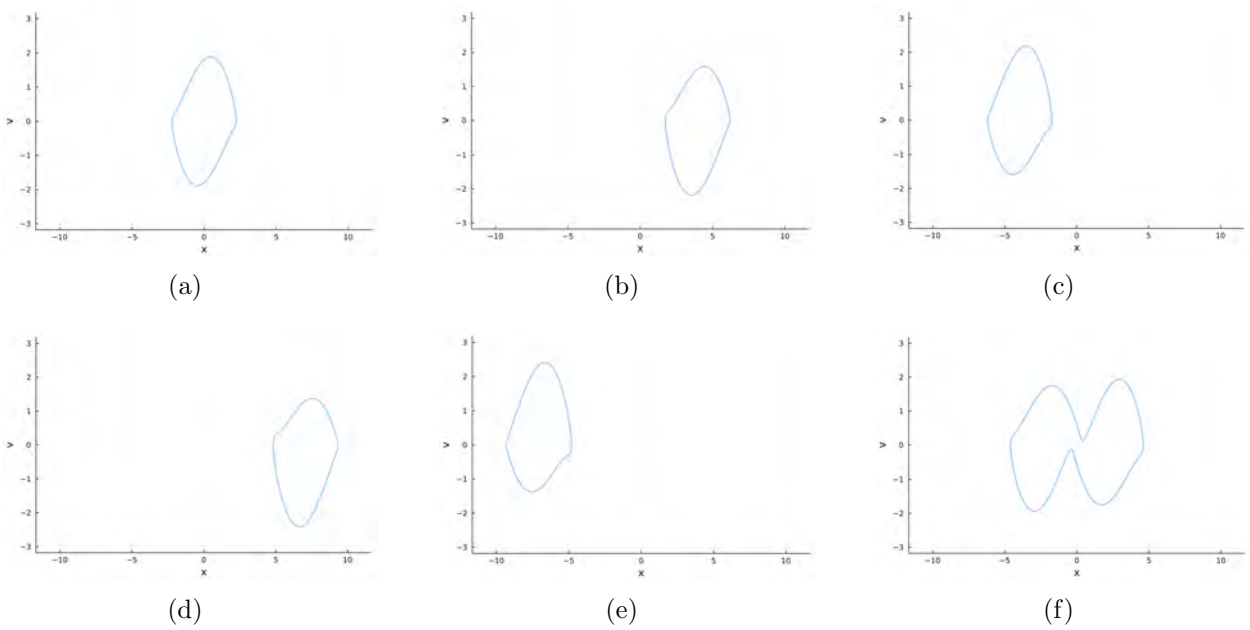

(a) (b) (c)

(d) (e) (f)

Figure 7: Numerical solution for the case $(k, k_0, \mu) = (0.05, 0.6, 0, 22)$, all plots being x against v. (a) $\mathcal{P}_1$, (b) $\mathcal{P}_2$, (c) $\mathcal{P}_3$, (d) $\mathcal{P}_4$, (e) $\mathcal{P}_5$, (f) $\mathcal{P}_6$

Periodic orbit	Floquet multipliers	Largest Floquet multiplier
$\mathcal{P}_1$	3.2793, 1.0476, -0.2780, -1.2571e-13	3.2793
$\mathcal{P}_2$	2.4471, 0.9999, 0.9983, 1.6773e-12	2.4471
$\mathcal{P}_3$	2.4471, 0.9999, 0.9983, 1.6773e-12	2.4471
$\mathcal{P}_4$	3.0235, 1.0050, 0.9992, 3.7006e-13	3.0235
$\mathcal{P}_5$	3.0235, 1.0050, 0.9992, 3.7006e-13	3.0235
$\mathcal{P}_6$	6.0027, 1.0032, 1.0032, -1.0620e-15,	6.0027

Table 2: Numerically computed Floquet multipliers using the method discussed in Subsection 3.2

5.3 Emergence of multimodal statistics

Taking the Poincaré section at $v = 0$ yields a set of points $y(t_i)$ such that $v(t_i) = 0$. In Figure 8 we display the probability density distribution of $x(t_i)$.

In figure 9 we we can see that as time steps are increased from 50000 to 500000, the

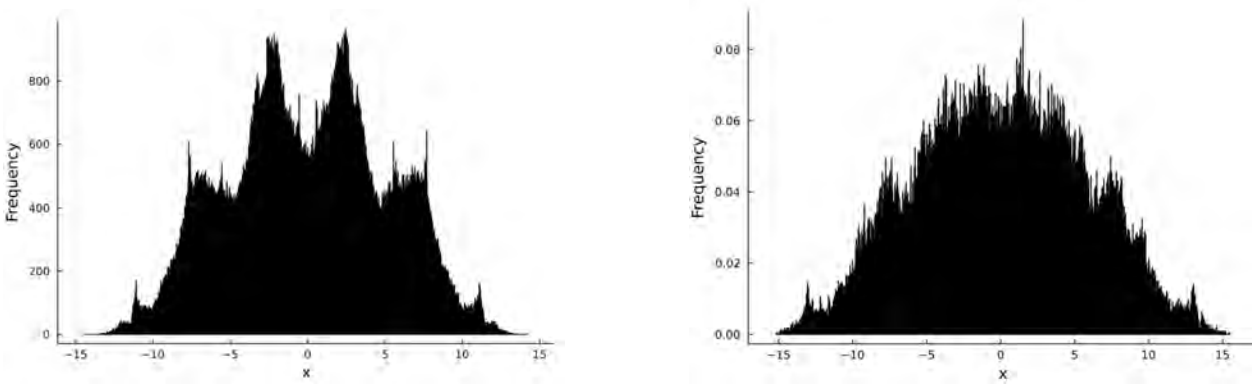

(a) (b)

Figure 8: Probability distribution functions position of turning points in a random walk like behavior (a) $(k, k_0, \mu) = (0.04, 0.6, 0.22)$ (b) $(k, k_0, \mu) = (0.05, 0.6, 0.22)$

distribution statistical distribution, which suggests that we must restrict our analysis to low time steps.

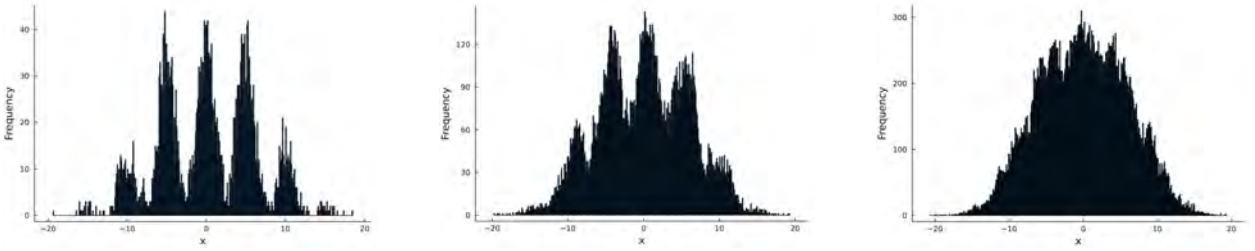

(a) (b) (c)

Figure 9: Probability distribution function of turning points in amn irregular walking regime at $(k, k_0, \mu) = (0.05, 0.8, 0.25)$. Plotted over (a) 50000 time steps (b) 100000 time steps (c) 500000 time steps

6 Discussion

Overall, we have been successful in understanding the effect of memory on both chaotic and non chaotic behavior, and hence providing a physical explanation for the transition between these kinds of behavior. Further, we have reported strong speed oscillations in the irregular walking regime which we justify appealing to the oscillatory nature of Equation 3.

In contrast to Durey's investigation of classical one dimensional pilot wave dynamics without a spring force [16], we have not observed any diffusive tendencies as time increases.

We have observed a plethora of UPO's during our numerical investigation, their shape and distribution being strongly dependent on the parameter values. Unfortunately, there does not seem to be a criteria to determine how many speed oscillations each shadowed periodic orbit has. Also, note that the values for the Floquet multipliers displayed in **??** and 2 are in line with Theorem 3.2 and Lemma 3.3, as we always get a multiplier fairly close to one an another one close to 0.

The main result we report from our stability analysis can be compressed in the following heuristic: The multimodal statistical tendencies strengthen when the Floquet multipliers of the shadowed unstable periodic orbits are low.

The major weak point in our study is that our approach to finding periodic orbits is not exhaustive. Given that we are implicitly using the trajectory to construct our guesses for any periodic orbit, if an orbit is too unstable it won't close, and hence it will not be detected by our algorithm. For instance, in Figure 10 we display a section of the droplet's trajectory in a chaotic walking regime.

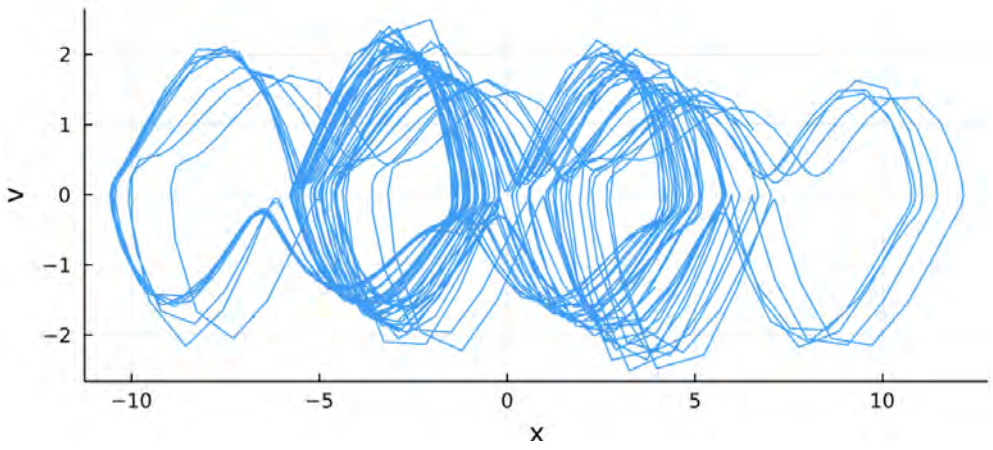

Figure 10: Position against velocity plot for the parameter case $(k, k_0, \mu) = (0.05, 0.6, 0.22)$

Continuing our Floquet multiplier stability analysis, future study could have a more local

perspective on transitions between unstable periodic orbits.

7 Practical takeaways

Nowadays, pilot wave dynamics are being studied as an interpretation of quantum mechanics, with a stringent focus on bridging quantum entanglement to dynamics of multiple droplets bouncing in the same wave field.

This is motivated from de Broglie's interpretation based upon particle-wave interaction, given that there is a wave function interacting with the droplet's movement. This non-Markovian dynamical system has a fundamental similarity with particle mechanics, bridging classical and quantum mechanics. The analogy has been explored through a series of experiments and theoretical explorations, summarized in Bush's review [22]. An example is Eddi et al. [23] experimental investigation of a walker traveling over a submerged barrier, which demonstrated that walkers exhibit similar features of quantum tunneling on a macroscopic scale. Also, Couder and Fort [24] reported that walkers exhibit single particle diffraction and interference when passing through apertures between submerged barriers; by sending single walkers toward a submerged barrier with openings on the scale of the guiding wavelength, it was observed that as the drop passed through the slit its trajectory was deviated. The distortion of its pilot wave against the boundary of the slit provides a macroscopic version particle diffraction.

Our research provides insight into this analogy, providing a consistent framework for the emergence of quantized behavior in the particle's trajectory. By studying the multimodal statistical distribution, we motivate seeking for a relationship between pilot wave mechanics under an added spring force and the quantum harmonic oscillator.

8 Acknowledgments

This research project would not have been possible without the support of several very special individuals and institutions, who I am delighted to acknowledge with the warmest gratitude and respect.

First and foremost, I would like to sincerely thank my mentor Nicholas Liu for his generous advice and assistance during this research, as well the head investigator of my research group, John M. Bush, for making my investigation possible. Likewise, I am indebted to my head mentor Dr. Tanya Khovanova and my tutor Dr. John Rickert for their valuable and insightful comments on my writing and presentation. My last week teaching assistant Yunseo Choi, as well as Dimitar Chakarov, have also provided helpful feedback on the final version of this paper. Prof. David Jerison and Ankur Moitra have provided valuable insight on my final oral presentation.

Further, I wish to express my gratitude to Executive Vice President Maite Ballestero, and the outstanding team of the Center of Excellence in Education (CEE) for giving me this life-changing opportunity to attend the 39th annual Research Science Institute, as well as Mr. Mark Kantrowitz and Yoland Gao for directing this progamme.

I also wish to pay tribute to the Massachusetts Institute of Technology (MIT) for providing the facilities for the research, as well as Dr. Maria Calsamiglia and Ms. Inma Ginés, the manager of Fundació Aula Escola Europea for sponsoring my stay at RSI.

Last not least, I am grateful to my family for their love and their unconditional support of my mathematical endeavors.

References

[1] J. Qian and C. K. Law. Regimes of coalescence and separation in droplet collision. *Journal of fluid mechanics*, 331:59–80, 1997.

[2] J. Miles. On faraday waves. *Journal of Fluid Mechanics*, 248:671–683, 1993.

[3] M. Durey and P. A. Milewski. Faraday wave–droplet dynamics: discrete-time analysis. *Journal of Fluid Mechanics*, 821:296–329, 2017.

[4] Y. Couder, S. Protiere, E. Fort, and A. Boudaoud. Walking and orbiting droplets. *Nature*, 437(7056):208–208, 2005.

[5] A. Eddi, E. Sultan, J. Moukhtar, E. Fort, M. Rossi, and Y. Couder. Information stored in faraday waves: the origin of a path memory. *Journal of Fluid Mechanics*, 674:433–463, 2011.

[6] D. M. Harris and J. W. Bush. Droplets walking in a rotating frame: from quantized orbits to multimodal statistics. *Journal of fluid mechanics*, 739:444–464, 2014.

[7] S. Perrard, M. Labousse, M. Miskin, E. Fort, and Y. Couder. Self-organization into quantized eigenstates of a classical wave-driven particle. *Nature communications*, 5(1):1–8, 2014.

[8] D. Viswanath. Symbolic dynamics and periodic orbits of the lorenz attractor. *Nonlinearity*, 16(3):1035, 2003.

[9] C. Grebogi, E. Ott, and J. A. Yorke. Unstable periodic orbits and the dimensions of multifractal chaotic attractors. *Physical Review A*, 37(5):1711, 1988.

[10] C. C. Maiocchi, V. Lucarini, and A. Gritsun. Decomposing the dynamics of the lorenz 1963 model using unstable periodic orbits: Averages, transitions, and quasi-invariant sets. *Chaos: An Interdisciplinary Journal of Nonlinear Science*, 32(3):033129, 2022.

[11] A. U. Oza, Ø. Wind-Willassen, D. M. Harris, R. R. Rosales, and J. W. Bush. Pilot-wave hydrodynamics in a rotating frame: Exotic orbits. *Physics of Fluids*, 26(8):082101, 2014.

[12] A. U. Oza, R. R. Rosales, and J. W. Bush. A trajectory equation for walking droplets: hydrodynamic pilot-wave theory. *Journal of Fluid Mechanics*, 737:552–570, 2013.

[13] R. N. Valani, A. C. Slim, D. M. Paganin, T. P. Simula, and T. Vo. Unsteady dynamics of a classical particle-wave entity. *Physical Review E*, 104(1):015106, 2021.

[14] J. Moláček and J. W. Bush. Drops walking on a vibrating bath: towards a hydrodynamic pilot-wave theory. *Journal of Fluid Mechanics*, 727:612–647, 2013.

[15] L. D. Tambasco and J. W. Bush. Exploring orbital dynamics and trapping with a generalized pilot-wave framework. *Chaos: An Interdisciplinary Journal of Nonlinear Science*, 28(9):096115, 2018.

[16] M. Durey. Bifurcations and chaos in a lorenz-like pilot-wave system. *Chaos: An Interdisciplinary Journal of Nonlinear Science*, 30(10):103115, 2020.

[17] R. Pino and G. E. Scuseria. Purification of the first-order density matrix using steepest descent and newton–raphson methods. *Chemical physics letters*, 360(1-2):117–122, 2002.

[18] P. Cvitanovic and Y. Lan. Proceedings of the 10th international workshop on multiparticle production: Correlations and fluctuations in qcd. 2003.

[19] M. Wu, Y. Xia, and Z. Xu. Floquet multipliers and the stability of periodic linear differential equations: a unified algorithm and its computer realization. *arXiv preprint arXiv:2201.04447*, 2022.

[20] R. Castelli and J.-P. Lessard. Rigorous numerics in floquet theory: computing stable and unstable bundles of periodic orbits. *SIAM Journal on Applied Dynamical Systems*, 12(1):204–245, 2013.

[21] V. T. ALAH. Numerical solution of fuzzy differential equation by adams-bashforth two-step method. 2004.

[22] J. W. Bush and A. U. Oza. Hydrodynamic quantum analogs. *Reports on Progress in Physics*, 84(1):017001, 2020.

[23] A. Eddi, E. Fort, F. Moisy, and Y. Couder. Unpredictable tunneling of a classical wave-particle association. *Physical review letters*, 102(24):240401, 2009.

[24] Y. Couder and E. Fort. Single-particle diffraction and interference at a macroscopic scale. *Physical review letters*, 97(15):154101, 2006.